Anat Embryol (2000) 201:407–417

ORIGINAL ARTICLE

Song-Lin Ding · Kathleen S. Rockland
De-Shu Zheng

Parvalbumin immunoreactive Cajal-Retzius and non-Cajal-Retzius neurons in layer I of different cortical regions of human newborn

Accepted: 20 October 1999

Abstract Neurons of layer I play an important role in the development of the basic structural and functional organization of the mammalian cerebral cortex. Basic data, however, concerning the spatial and temporal distribution of the neuron populations in layer I are still limited, especially for human material. The present study investigates the distribution of Cajal-Retzius (CR) and non Cajal-Retzius (NCR) neurons in thirteen cortical areas in the newborn human in terms of their relative density and possible subtypes. Neuronal populations were identified by immunohistochemistry for parvalbumin. Three main results are reported. First, parvalbumin-immunoreactive (Parv-ir) CR cells were observed in all of the neocortical areas examined. These areas also had a Parv-ir horizontal fiber plexus in deep layer I, confirming to the horizontal plexus classically associated with CR neurons. Second, many Parv-ir CR cells showed clear signs of degeneration. Third, in addition to the large CR cells, smaller Parv-ir NCR neurons occurred in many of the neocortical areas examined. These were morphologically heterogeneous and may represent several subtypes. By sampling across several areas, we were able to establish that these NCR cells occurred at higher density in primary sensory areas 3, 1, 17, and 41. Because of this variability in density of Parv-ir NCR cells, the ratio of Parv-ir CR to Parv-ir NCR cells is selectively lower in primary sensory areas. Recent investigations in somatosensory cortex of early postnatal rat report complex spatiotemporal patterns of correlated spontaneous activity among neurons in layer I (Schwartz et al. 1998). An interesting possibility is that regional variability in this activity may play a major role in the organization of cortical circuitry in different areas.

Key words Calcium-binding protein · Neocortex · Cortical Development · Interneuron · Immunocytochemistry

S.-L. Ding (✉) · D.-S. Zheng
Institute of Neuroscience, Guangzhou Medical College, Guangzhou 510182, People's Republic of China

K.S. Rockland
Department of Neurology, University of Iowa, College of Medicine, Iowa City, IA 52242, USA

Present address:
S.-L. Ding, Department of Neurology, University of Iowa, 200 Hawkins Drive, Iowa City, IA 52242, USA
e-mail: slding@blue.weeg.uiowa.edu
Tel.: (319)335-6524, Fax: (319)356-4505

Introduction

Neurons of layer I play an important role in the development of the basic structural and functional organization of the mammalian cerebral cortex. The distinctive population of Cajal-Retzius (CR) cells is implicated in cell migration, cortical lamination, and possibly gyral formation (reviewed Frotscher 1998; Marin-Padilla 1998; Meyer and Goffinet 1998; Super et al. 1998). There is also a second, more numerous population of smaller non-Cajal Retzius (NCR) neurons. These have recently been reported to engage in complex spatio-temporal patterns, which may actively influence the formation of cortical circuitry (Schwartz et al. 1998).

Despite the considerable interest of these processes, basic data concerning the spatial and temporal distribution of these two populations in layer I are still limited, especially for NCR cells in humans. Moreover, some findings about CR cells remain controversial, probably related to the relatively small samples and the use of different histological protocols. In visual cortex of the human newborn, for example, the number of parvalbumin-immunoreactive (Parv-ir) CR cells has been reported as large by some investigators (Ding et al. 1998) but much smaller by others (Cao et al. 1996).

The present study investigates the distribution of Parv-ir neurons in layer I of thirteen cortical regions in the brain of the newborn human. It addresses the relative densities of Parv-ir CR and Parv-ir NCR neurons, and their possible morphological subtypes. Parvalbumin (Parv) was chosen as a marker because of the Golgi-like

detail of staining, because we found Parv but not calbindin (CalB) to be expressed by CR neurons in the newborn (Ding et al. 1996, 1997, 1998), and because of its interest as a neuroprotective molecule (see Heizmann and Braun 1995). An additional goal was to investigate morphological signs of degeneration and cell death in the CR population, as evidence of their developmental fate.

Materials and methods

Three human newborn specimens at 38 (one case) and 39 (two cases) gestational weeks (GW; determined by maternal history and crown-rump length) were obtained after neonatal death from non-neurological causes. Procedures were in accordance with Chinese legislation and were supervised by the Ethical Commitee of the Hospital, Guangzhou, China. The specimens showed no gross malformations; and no clinical history of family-linked neurologic disorders was reported. The specimens were perfused transcardially with saline within 2 h after death, followed by 3.5 l of 4% paraformaldehyde in 0.1 M phosphate buffer (PB, pH 7.3, 4°C). The brains were removed and postfixed in the same fixative overnight at 4°C; and 5.0–6.0 mm-thick tissue blocks were then excised from different cortical regions. Blocks from the precentral, postcentral, middle frontal, superficial temporal, Heschl's, and parahippocampal gyri and the calcarine fissure were dissected as shown in Figure 1. Blocks were cut perpendicular to the long axis of the calcarine fissure (for visual cortex) or (for other blocks) perpendicular to the long axis of the neighboring gyri (see Fig. 1). The excised regions were planned to correspond, respectively, to cortical areas 4, 3-1-2, 46, 22, 41-42, 28-35-36 plus the hippocampal formation, and areas 17 and 18, as located in relation to major sulcal landmarks. The blocks were soaked in 10%, 15% and 30% sucrose in PB sequentially until the tissues sank, and then were sectioned at 40 µm with a cryostat. Two sets of sections from each block were collected: one for Nissl staining, and the other for Parv-ir.

For immunohistochemistry, sections were preincubated in PB containing 5% normal goat serum (NGS) and 0.1% Triton X-100 for 1 h at room temperature (RT). The sections were then incubated in PB containing mouse monoclonal anti-Parv antibody (1:8000, Celio et al. 1988) for 24 h at 4°C. They were rinsed in PB and transferred to a solution containing biotinylated goat anti-mouse IgG (1:100, Elite kits, Vector Labs, Burlingame CA) for 1 h at RT. Immunoreactivity was visualized with avidin-biotinylated HRP (ABC kit, Vector) and HRP histochemistry, with 3,3′-diaminobenzidine tetrahydrochloride (DAB) as the chromogen. The sections were then washed, dehydrated, cleared with xylene, and coversliped with DPX. As a control for non-specific staining, the above processes were repeated on additional sections except that the primary antibody was replaced by NGS. No immunostaining was found under these conditions.

Analysis

The identity of cortical regions was determined by the gross topographic location of the tissue blocks (see Fig. 1) and the cytoarchitectonic features of Nissl-stained sections. The lower border of layer I was easily determined by the markedly higher packing density of neurons in layer II, as visualized by Nissl stains or Nomarski optics. The packing density of Parv-ir CR and Parv-ir NCR cells in different areas of the 38 GW case was derived by charting labeled neurons (Parv-ir CR and NCR cells) in layer I under 2.0 mm of pia surface with a camera lucida microscope attachment (at ×200 magnification). The length of 2.0 mm was chosen because of the scattered distribution of the CR cells, and to allow comparison with other studies in which a similar method were used. Cells were counted in four sections from each area and the mean values were expressed as "under 2.0 mm of pia surface." This semi-quantitative method follows guidelines for populational ratios (Saper 1996), and was adopted to facilitate comparisons with previous related work on CR cells during prenatal development (Meyer and Goffinet 1998).

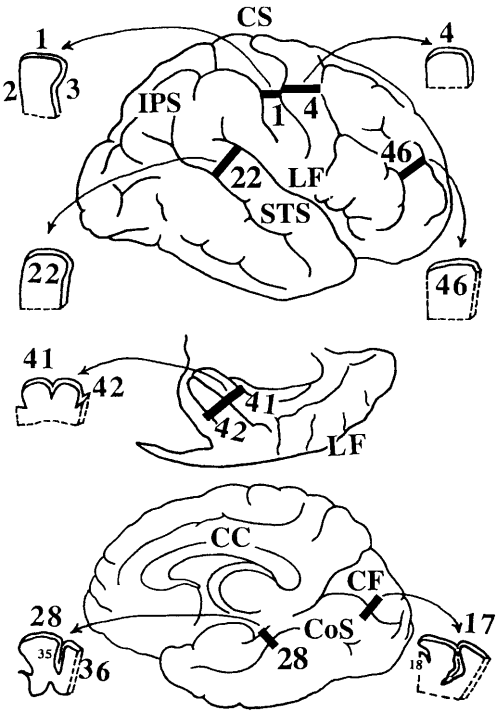

Fig. 1 Schematic diagrams of the lateral surface, exposed Heschl's gyrus, and medial surface of the cerebral hemisphere of the newborn to show the general location of the excised tissue blocks (architectonic areas are indicated by numbers). The shapes of the blocks as shown are from the 38 GW case (*CC* corpus callosum, *CF* calcarine fissure, *CoS* collateral sulcus, *CS* central sulcus, *IPS* intraparietal sulcus, *LF* lateral fissure, *STS* superior temporal sulcus)

Results

All the neocortical areas examined contained Parv-ir neurons scattered through different layers besides layer I, as previously reported elsewhere (Yan et al. 1993 and see example in Fig. 2A–D). The present study concentrated on the cell types and regional distribution of Parv-ir neurons specifically in layer I. Only the neocortical areas are described since no Parv-ir neurons and fibers were detected in layer I of the hippocampus and subicular complex. Two basic categories of Parv-ir neurons could be distinguished in layer I of the human newborn; namely, Parv-ir CR neurons and Parv-ir NCR neurons.

Parv-ir CR neurons

Large Parv-ir neurons (12–35 µm in diameter) were observed in layer I of all the 12 sampled neocortical areas and the entorhinal cortex (area 28). These large Parv-ir cells were localized in the upper half of layer I, and had all the morphological characteristics of typical CR cells (see Figs. 2A, F–H, 3), as previously described in the hu-

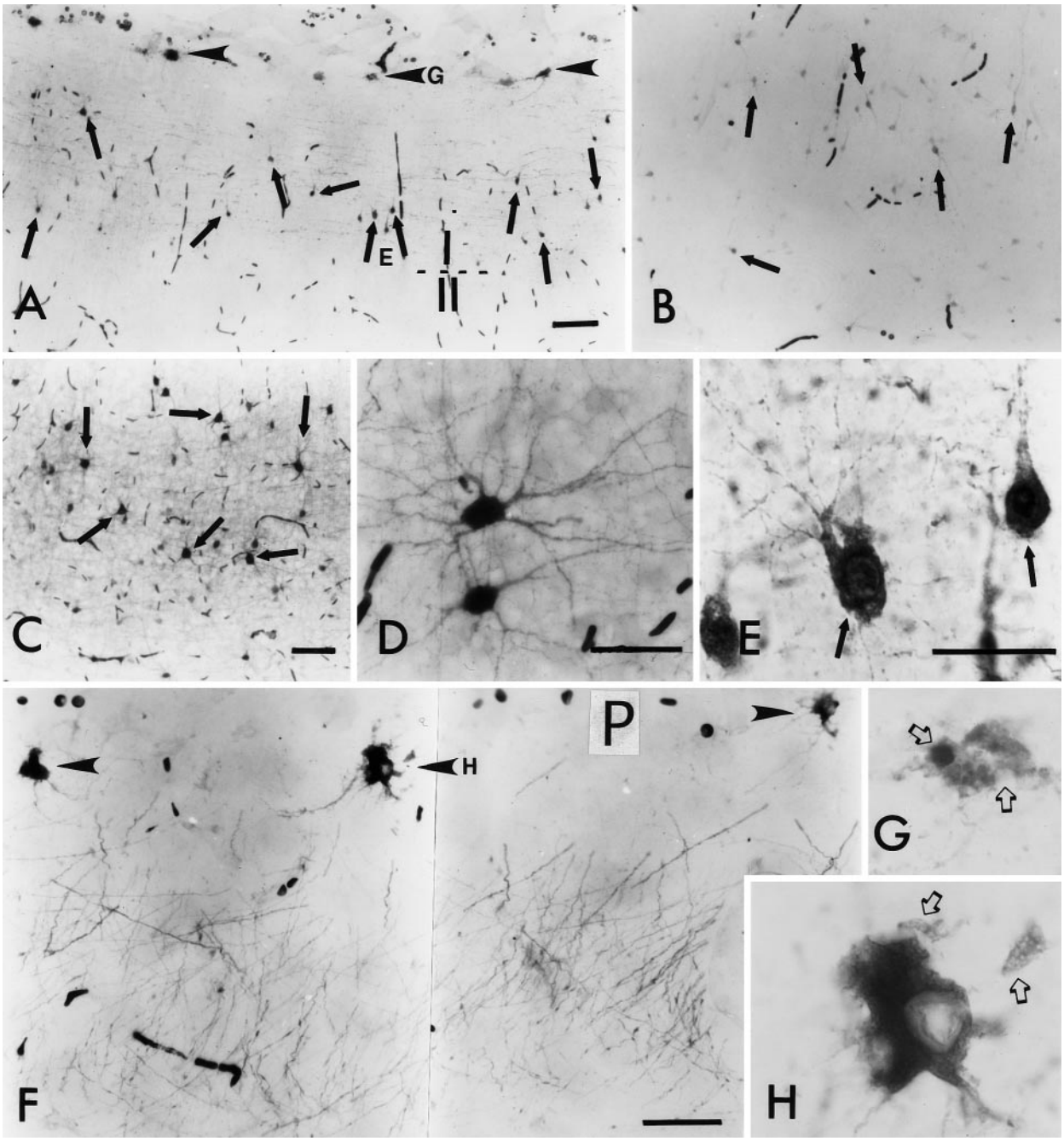

Fig. 2 Distribution and morphology of Parv-ir neurons in the primary sensory cortex, area 3 (**A**, **C**–**E**, **G**) and the association cortex, area 22 (**B**, **F**, **H**). **A** Distribution of Parv-ir CR and NCR cells in layer I of area 3. Note the location of Parv-ir CR cells (*arrowheads*) and NCR cells (*arrows*), and the density of Parv-ir NCR cells in area 3. Two of the NCR cells (at *arrows marked E*) and one of the CR cells (at *arrowhead G*) are shown at higher magnification in **E** and **G**, respectively. The pia is to the top; the dashed line marks the border of layers I and II (same convention throughout in other figures). *Bar* 100 µm. **B**, **C** Distribution of Parv-ir neurons (*arrows*) in the deep layers of area 22 (**B**) and area 3 (**C**). *Bar* 100 µm. **D** Detailed morphology of two larger Parv-ir cells from layer IV of area 3 to demonstrate normal (i.e., non-degenerating) appearance. *Bar* 40 µm. **F** Parv-ir CR cells and fibers in layer I of area 22. The CR cells (*arrowheads*) seem to be aligned at regular intervals; no Parv-ir NCR cells were observed in this region. One of the CR cells (at *arrowhead H*) is shown at high power in **H** (*P* pia). *Bar* 50 µm. **E**, **G**, **H** Higher magnification photomicrographs show the morphology of Parv-ir NCR cells (**E**) and CR cells (**G**, **H**). Note that the two CR cells (**G**, **H**) display obvious signs of degeneration (*open arrows*). These include shrunken and broken cell bodies (**G**), fragmentation or loss of processes (**G**, **H**), and twisted and vacuolated dendrites (**H**). *Bar* 20 µm

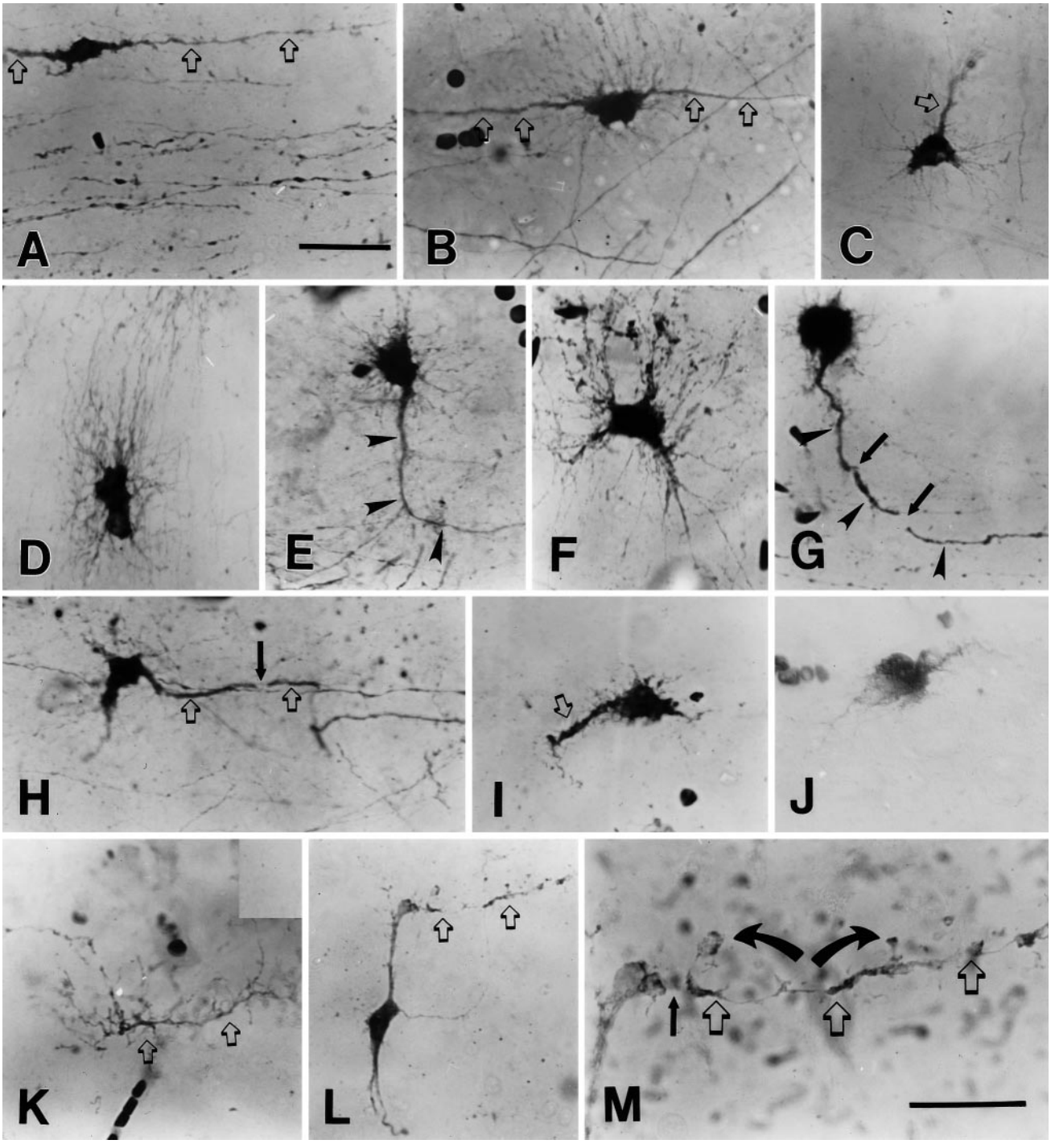

Fig. 3A–M Detailed morphology of Parv-ir CR cells showing different soma shapes, as well as signs of degeneration. Some of the dendrites (*open arrows*) and axons (*arrowheads*) of the CR cells are indicated. Frequently observed signs of degeneration of CR cell included disconnection of vertical dendritic branchlets (*curved arrows* in **M**) from the pia (**A**, **K**, **L**, **M**), profuse outgrowth of hairy appendages from cell bodies (**B**, **D F**), broken processes (*solid arrows* in **G**, **H**, **M**), contorted and twisted dendrites (**I**), and vacuolated cell bodies (**C**, **I**, **J**). *Bar* **A**–**L** 40 µm; **M** 20 µm

man and subhuman primates by Cajal (see DeFelipe and Jones 1988) and many other investigators (Marin-Padilla and Marin-Padilla 1982; Marin-Padilla 1990; Huntley and Jones 1990; Meyer and Gonzalez-Hernandez 1993; Verney and Derer 1995; Yan et al. 1995).

No obvious differences in the morphological appearance of Parv-ir CR cells were found across the cortical areas sampled, but their density varied slightly in different regions. Areas 46 and 28 had the lowest density of cells (1–3 cells under 2.0 mm of pia surface) and areas 22 and 3 had the highest density (4–8 cells under 2.0 mm

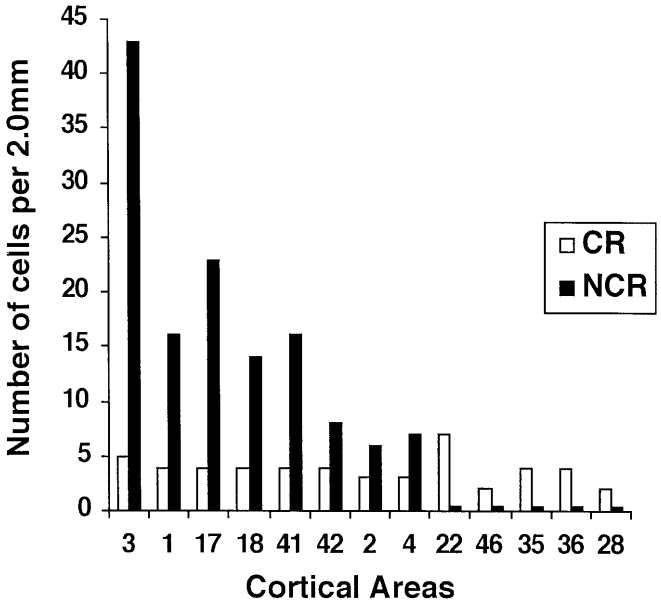

Fig. 4 Histogram showing the density of Parv-ir CR and NCR neurons in layer I under 2.0 mm of pia surface in 13 different cortical areas of the newborn human

of pia surface; Figs. 4, 5). Overall, more Parv-ir CR cells were observed along the depths of the sulci (in the lateral fissure, superior temporal sulcus, and collateral sulcus) than along the convex portions of the gyri (Fig. 5). This observation was not universal, however, as there was no obviously uneven distribution of Parv-ir CR cells along the depth of the central and postcentral sulci (areas 3 and 2) or the convexity of the postcentral gyrus (area 1).

Most of the Parv-ir CR cells in the newborn displayed various signs of degeneration (Figs. 2, 3). What are presumed to be earlier signs include shrunken and vacuolated cell bodies and dendrites (Figs. 2F, H; 3C, I, J), disconnection of vertical dendritic branchlets from the pia (Fig. 3A, K, L), contorted and twisted dendrites (Figs. 2H; 3I), profuse outgrowth of hairy appendages from cell bodies (Fig. 3B, D), and dendritic and axonal processes of broken appearance (Fig. 3G, H). The later signs include fragmentation or loss of dendritic and axonal processes (Fig. 3G, L, M), broken cell bodies, and lightly stained membranous debris (Fig. 2G).

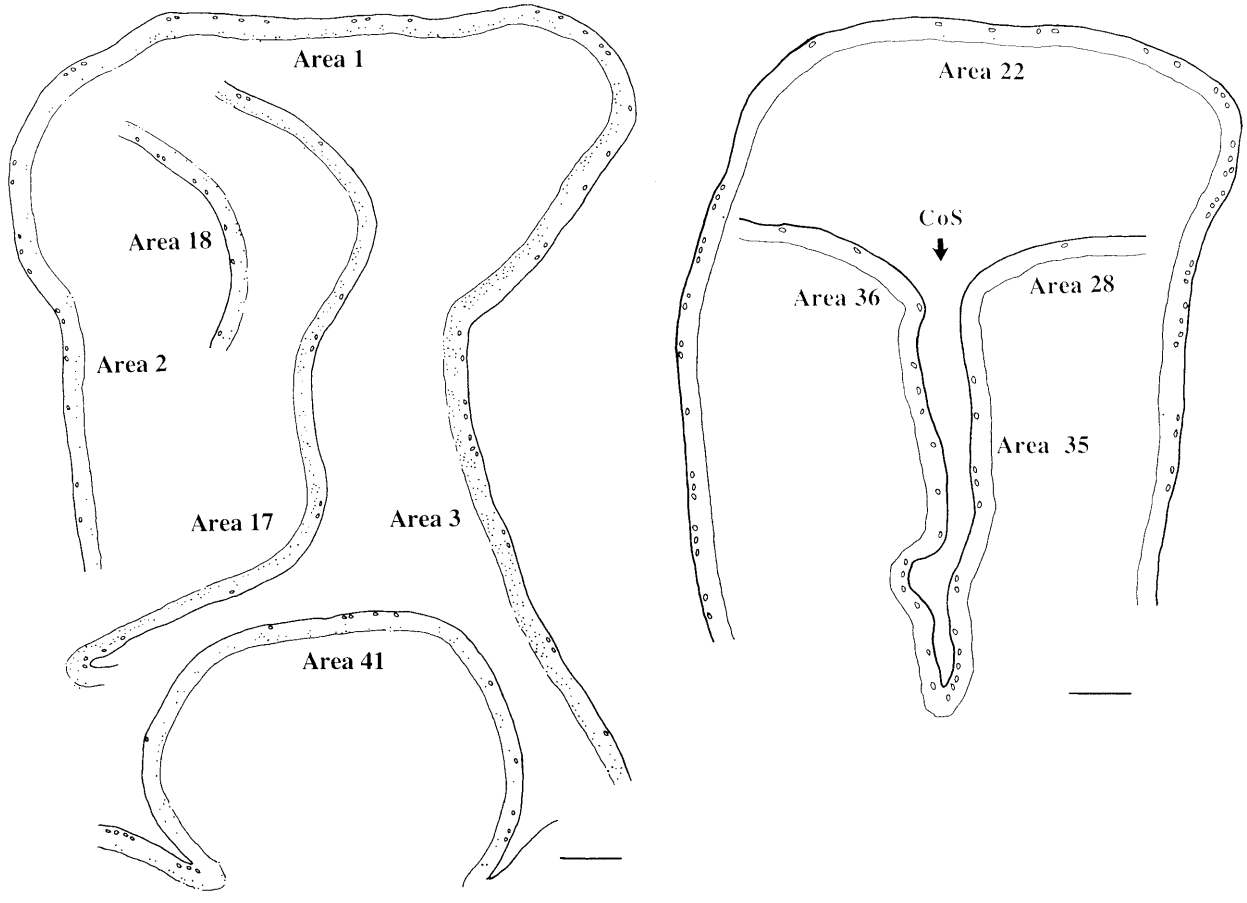

Fig. 5 Camera lucida drawings from the 38 GW case showing the distribution and density in layer I of Parv-ir CR cells (*larger, open circles*) and NCR cells (*smaller dots*) in areas 3, 1, 2, 17, 18, 41, 22, 28, 35 and 36. See Fig. 1 for general location of excised tissue blocks. *Bars* 1.0 mm

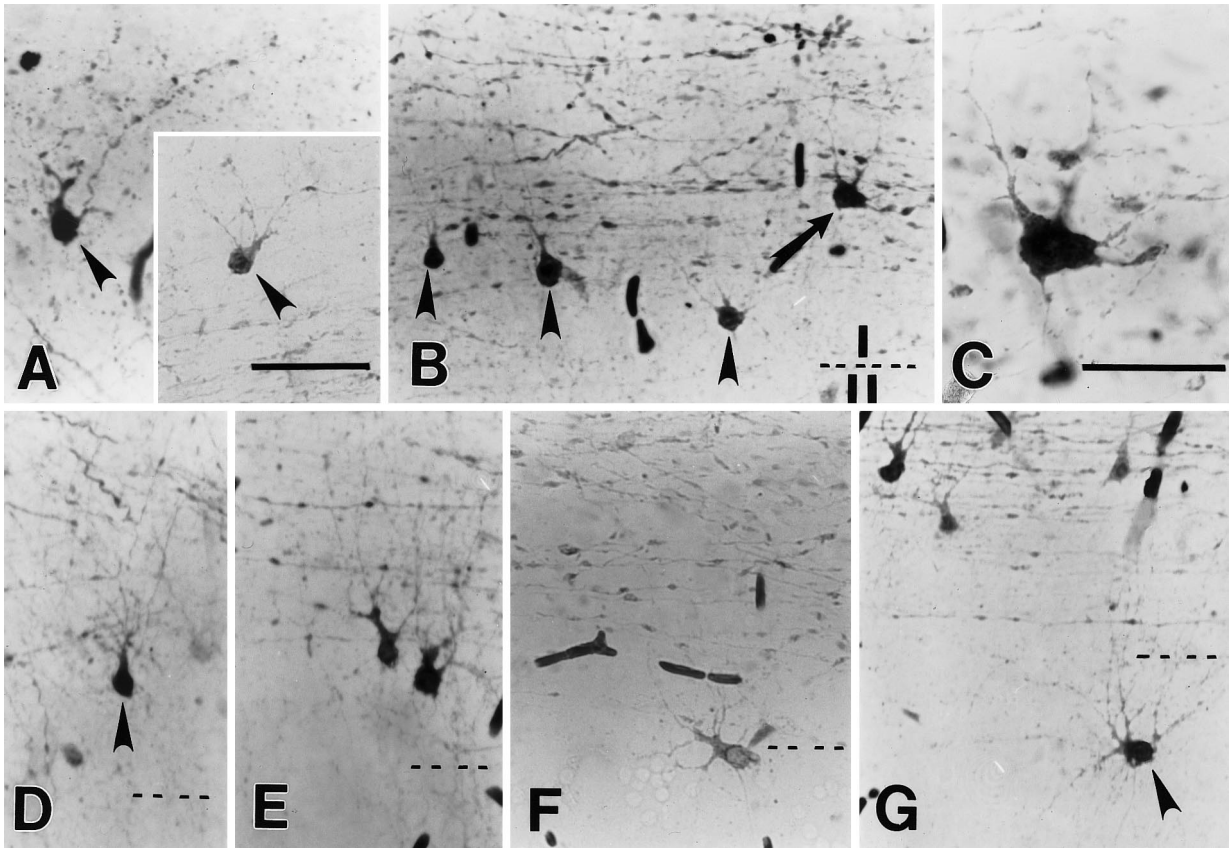

Fig. 6A–G Distribution and morphology of Parv-ir NCR cells in layers I and II. **A** and **Inset** Parv-ir NCR cells (*arrowheads*) in the upper part of layer I of area 3. **B**, **C** Parv-ir NCR cells in deep layer I of area 17. Note that most of these cells have pyramid-shaped somata with ascending dendrites (*arrowheads*), but one (*arrow*, and at higher magnification in **C**) appears more multipolar in shape. **D** A Parv-ir pyramid-shaped NCR cell (*arrowhead*) in deep layer I of area 41. **E**–**G**: Parv-ir NCR cells from area 17 occur variably in the deep part of layer I (**E**), at the border of layers I/II (**F**), or within layer II (*arrowhead* in **G**. *Bar* **C** 20 µm; others 40 µm

Parv-ir NCR neurons

Several types of smaller Parv-ir neurons occurred in layer I of areas 3, 1, 17, 18, 41, 42, 4, and 2. These neurons are easily distinguished from Parv-ir CR cells by the much smaller size of their soma (5–12 µm in diameter), their dendritic morphology, and their preferential location in the deeper half of layer I (Figs. 2A, E; 6, 7). Consistent with previous reports of NCR cells in human motor cortex and in the neocortex of other species (Bradford et al. 1977; Marin-Padilla 1984; Cajal-Agueras et al. 1989; Anderson et al. 1992; Prieto et al. 1994; Hestrin and Armstrong 1996; Zhou and Hablitz 1996), we observed what appeared to be at least three morphologically distinct subtypes. The majority of Parv-ir NCR cells had a pyramid-shaped soma with a thick primary ascending denrite, which branched into several thin second- or third-order dendrites (Figs. 6, 7). One to three additional thinner dendrites usually extended from the soma. Dendrites of this cell type were beaded but spine-free, extended radially or obliquely toward the pia, and intermingled with or crossed through the horizontal fiber plexus in deep layer I (Figs. 6, 7). Axons from this cell type were often seen descending from the base of the soma (Fig. 7). Some of these could be followed into layers II or III (Fig. 7B); but others seemed to be confined to layer I (Fig. 7A).

Parv-ir NCR cells in upper layer I may be another distinct subtype (Fig. 6A). These cells had heavily beaded dendrites and were often darkly stained, although axonal processes were hard to distinguish. These cells often showed signs of degeneration, and had punctate, dustlike debris in their vicinity. Only a few of these more superficial neurons were detectable in the newborn. A few Parv-ir stellate and multipolar cells (without thick primary asecnding dendrites as compared to the pyramid-shaped cell type) were also observed in layer I (Figs. 6C; 7C, D), but there were no bipolar or bitufted Parv-ir NCR cells.

No obvious differences in the morphologies of Parv-ir NCR cells were found in the separate neocortical areas; but, in contrast with Parv-ir CR cells, the distribution and density of Parv-ir NCR neurons varied greatly (Figs. 2, 4, 5). The highest density of Parv-ir NCR cells occurred in area 3 (40–46 cells under 2.0 mm of pia surface); and the next highest, in area 17 (22–25 cells), area 1 (15–17 cells), area 41 (15–17 cells), and area 18 (13–16 cells). There was a much lower density of Parv-ir NCR cells, scattered in the deep half of layer 1, in areas 4, 2, and 42 (6–8 cells); and only a few occasional Parv-ir

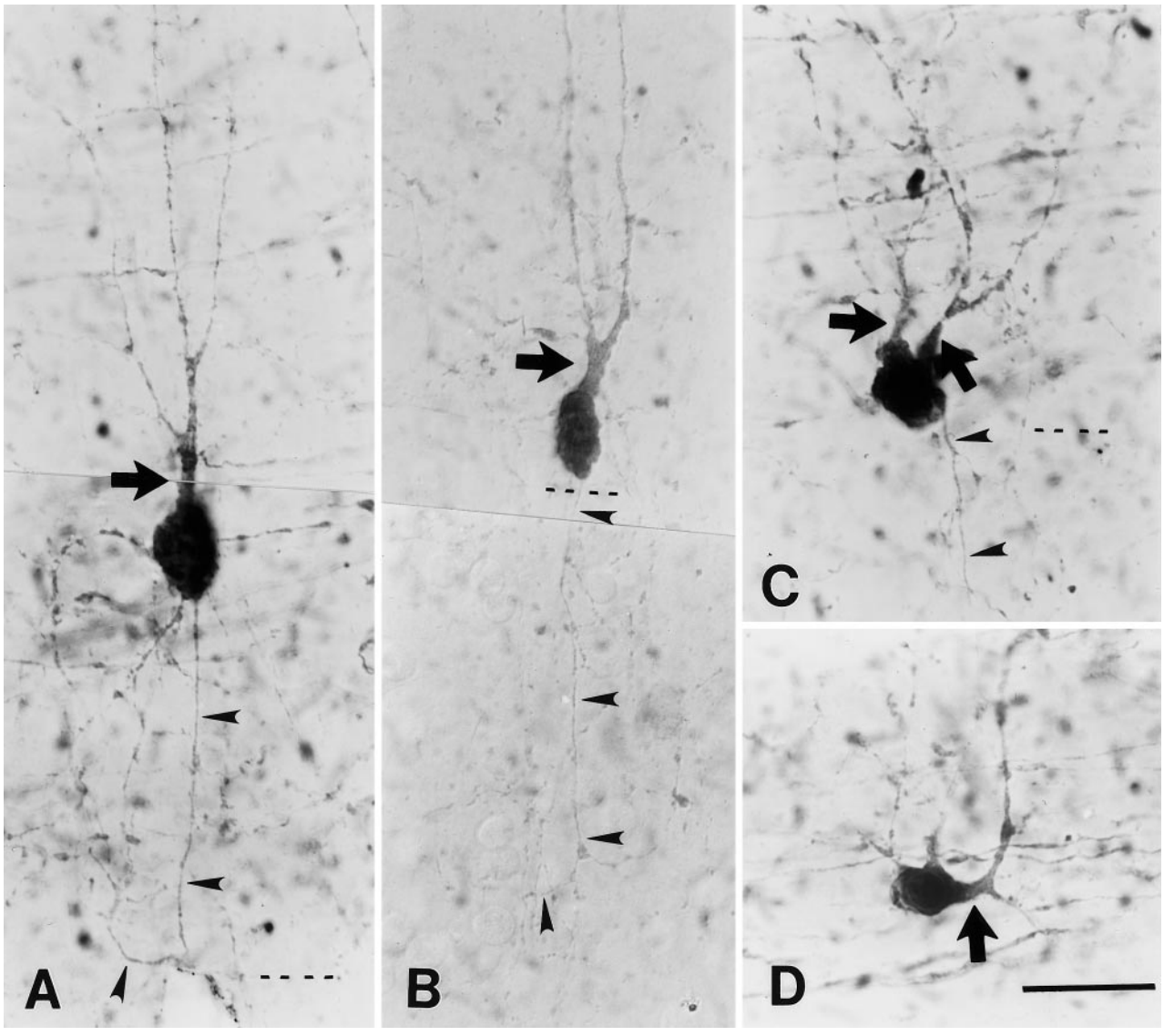

Fig. 7 Examples of what appear to be different cell types of Parv-ir NCR cells in the deep half of layer I of area 3 (**A**, **B**) and area 17 (**C**, **D**). **A**, **B** Pyramid-shaped Parv-ir NCR cells with ascending dendrites (*arrow*) and descending axons (*arrowheads*). The axons extend within layer I (**A**) or into layers II and III (**B**). **C**, **D** Two examples of other types of Parv-ir NCR cells. One of them (**C**) also extends an axon into deeper layers. *Arrows* mark the main dendrites; *small arrowheads* mark axons. *Bar* 20 μm

NCR neurons in areas 22, 28, 35, 36, and 46. In regions of higher density, mamy Parv-ir NCR neurons had darkly stained processes; but in regions of lower density, they tended to be more lightly stained. Sometimes Parv-ir NCR cells at the border region between layers I and II were aligned at regular intervals of about 100 μm.

Parv-ir layer I fibers

A dense plexus of mostly horizontal Parv-ir fibers occurred in the deep part of layer I of all the neocortical areas investigated, both in areas with high (areas 3, 1, 17, 18 and 41) and low density of Parv-ir NCR neurons (Figs. 2A, F, 6B, F, 8A). Fewer Parv-ir fibers were detectable, however, in the entorhinal cortex, area 28, where there were fewer Parv-ir CR cells.

At least two types of Parv-ir fibers were distinguishable. One had a larger diameter and few varicosities, and was located mainly in the upper part of the plexus; the second had a smaller diameter and many varicosities, and was located deeper in the plexus (Fig. 8A).

Some horizontally oriented Parv-ir fibers at the border of layers I and II were tipped with growth cone-like structures. In addition, there were a few vertical Parv-ir fibers between layers I and II which were often tipped with growth cone-like structures (Fig. 8B, C). Finally, in area 17 but not in other areas, a few vertical Parv-ir fibers, often lightly stained and ending in growth cone-like tips, were visible traveling from layers II and III toward the pia.

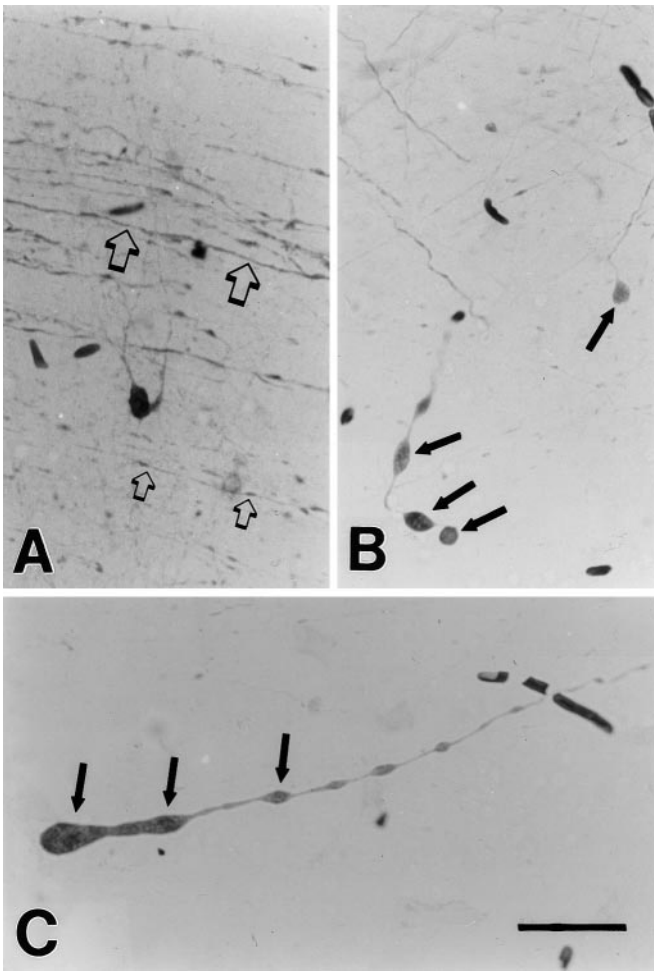

Fig. 8 A Large and small caliber Parv-ir fibers (indicated by *large* and *small arrows*, respectively) in the deep half of layer I. **B**, **C** Vertical (**B**) and horizontal (**C**) Parv-ir fibers tipped with growth cone-like and varicose structures (*solid arrows*). *Bar* 40 µm

Discussion

During development, neurons in layer I participate in processes of neuronal migration and laminogenesis, among other functions possibly related to gyral formation of the establishment of connections (reviewed Frotscher 1998; Marin-Padilla 1998; Super et al. 1998; Meyer and Goffinet 1998). Layer I shares a common ontogenetic history, as the primordial plexiform layer of the pre-cortical plate, with the subplate, whose neurons also play a critical role in neuronal migration and the establishment of connections (Finney et al. 1998; Super et al. 1998). In contrast with the subplate, however, the structural and functional organization of layer I has been much less investigated.

In the present investigation of layer I, we report the persistence of Parv-ir CR cells in thirteen cortical areas in the newborn human, in addition to the occurrence of Parv-ir NCR cells. By sampling across several areas, we were also able to identify differences in the distribution of Parv-ir NCR cells and, by extension, in the ratio of Parv-ir CR to Parv-ir NCR cells.

Parv-ir CR cells

At mid-gestation, most CR cells in humans are reported to contain calbindin-D28k (CalB) and calretinin (CalR; Verney and Derer 1995; Yan et al. 1997; Ding et al. 1996, 1997). A few CR cells show immunoreactivity for Parv at midgestation (Verney and Derer 1995; Cao et al. 1996; Ding et al. 1996, 1998), but more Parv-ir CR cells appear later, after 30 GW (Ding et al. 1996, 1998). This appears to complement the time course of expression for CalB, which, in contrast, peaks from 15–16 GW to 28–30 GW (Ding et al. 1996, 1997; Yan et al. 1997).

There have been previous reports of Parv-ir CR cells at later developmental stages, but the results have been inconsistent (Cao et al. 1996; Ding et al. 1996, 1998). In visual cortex of the human newborn, for example, the number of Parv-ir CR cells has been reported as large by some investigators (Ding et al. 1998) but much smaller by others (Cao et al. 1996). Several reasons may account for the discrepancies, including technical differences in the immunohistochemistry (i.e., the primary antibodies in particular), variability owing to the small sample sizes, and variability in the exact choice of areas sampled. The persistence of Parv-ir CR cells in the newborn, as reported here, is corroborated by the plexus of Parv-ir horizontal fibers. These Parv-ir fibers most likely correspond to axons of Parv-ir CR cells for the following reasons: (1) they extended horizontally for a very long distance exclusively in the deep layer I – this is a defining feature of the axonal plexus of CR cell in humans (Marin-Padilly 1984; 1990); (2) fibers were not found in layer I of the hippocampus and subiculum, where no Parv-ir CR cell bodies were seen (Yan et al. 1993; Ding et al. 1999); (3) they are probably not thalamocortical projecting axons since they were found in both primary sensory and association neocortices (see Fig. 2), although Parv-ir thalamocortical axons mostly terminate in layers IV and deep III of the primary sensory cortices (Hashikawa et al. 1995).

Parv is probably not co-expressed with CalB, CalR or reelin in the CR cells of the human newborn since no CalB-ir CR cells and only a few small to medium-sized horizontal CalR-ir and reelin-ir neurons has been found in layer I at this stage (Ding et al. 1996, 1997; Yan et al. 1997; Letinic and Kostovic 1998; Meyer and Goffinet 1998). However, It is possible that Parv might colocalize with AChE in CR cells at this stage since AChE-containing CR cells has been described in human auditory cortex at birth (Krmpotic-Nemanic et al. 1987).

The density of Parv-ir CR cells in the newborn is much reduced in comparison with the density of reelin-ir CR cells at earlier stages. We found <8 Parv-ir CR cells under 2.0 mm of pia surface, versus the 80 (at 16–17 GW) and 30–40 (at 27 GW) reelin-ir CR cells under 1.3 mm of pia surface, reported by Meyer and Goffinet (1998). This difference suggests that the Parv-ir CR cells persisting in the newborn are a small subset of the larger population of earlier stages. Consistent with this interpretation, most of the Parv-ir CR cells showed some of the standard features of degeneration.

Although consistent with other reports (Meyer and Gonzalez-Hernandez 1993; Huntley and Jones 1990; Hendrickson et al. 1991; Meyer and Goffinet 1998; Super et al. 1998), there is some possibility that what we are interpreting as signs of degeneration could be artifacts, in particular due to changes between the time of death and fixation. The brain tissues used in the present study, however, were perfused within two h after death; and a previous study, at both the light and electron microscopic levels, indicates that Parv-ir and CalB-ir neurons in human hippocampal formation were morphologically well preserved in brains perfused within 2 h after death (Seress et al. 1993). Moreover, in our present and previous studies (Yan et al. 1993; Ding et al. 1998, 1999), Parv-ir neurons in other layers besides layer I did not show any clear signs of degeneration (see Fig. 2D). Finally, the interpretation of degenerating CR cells is consistent with the observation that only a few widely scattered presumptive CR neurons, of the horizontal bipolar form, are found in the adult cerebral cortex (Marin-Padilla 1984, 1990; Meyer and Gonzalez-Hernandez 1993; Belichenko et al. 1995; Fonseca and Soriano 1995; Gabbot et al. 1997; Meyer and Goffinet 1998).

Parv-ir NCR cells

NCR cells in layer I have been characterized in Golgi preparations as belonging to three categories (Marin-Padilla 1984): NCR cells with rich axonal plexuses that extend into layer II; NCR cells with poor axonal arborizations; NCR cells with indistinguishable axonal and dendritic arborizations. The present study demonstrates the existence of many Parv-ir NCR cells in deep layer I of areas 3, 1, 17, 18, 41, 42, 4 and 2. In these areas, most Parv-ir NCR neurons had a pyramid-shaped soma with ascending primary dendrite and descending axon. From these neurons some axons could be followed into layers II and III, while others seemed confined within layer I. A few Parv-ir NCR seemed to belong to other, neuroglia-form or multipolar subtypes, as based on dendritic configuration. The axons of these cells tended not to be clearly labeled.

The present report, for the first time, indicates that the density of Parv-ir NCR cells in layer I of the newborn varies greatly among different cortical areas, with the highest density being in the primary sensory cortices, and the lowest density in the association cortices. Other studies in the rat, cat and human have similarly reported that populations of Parv-ir neurons in primary somatosensory, visual, and auditory cortices differentiate earlier than those in other cortical areas (Alcantara et al. 1993; Yan et al. 1993; Alcantara and Ferer 1994; Ding et al. 1996).

The development of Parv expression has been suggested to correlate with the functional maturation of a given area (see Alcantara and Ferer 1994). As another indicator of maturation, comparative synaptogenesis in different areas of the human brain shows that synapses in primary auditory cortex (Heschl's gyrus) appear earlier than those in prefrontal association cortex (Huttenlocher and Dabholkar 1997).

Few or no Parv-ir NCR cells have been reported in layer I of the human adult (Blumcke et al. 1990; Hof et al. 1995). As has been suggested for Parv-ir CR cells, the reduced numbers of Parv-ir NCR cells between the newborn and adult may be the consequence of cell death, since there were also signs of degeneration within this population in the newborn (the present study). Cell death or cell loss has been found for immature neurons including cells in the proliferative zone in humans and other species (e.g., Klekamp et al. 1991; Thomaidou et al. 1997). Alternately or additionally, these neurons may persist but express other chemicals, such as CalR, in the adult. Large numbers of CalR-ir NCR cells have been observed in layer I of the adult (Del-Rio and DeFelipe 1996). Another possibility is that some of the Parv-ir NCR cells may shift into layer II (see Fig. 6).

Functional significance

Layer I and CR cells in particular are known to play important roles during development in cell migration, laminogenesis, and axon guidance (reviewed Frotscher 1998; Marin-Padilla 1998; Super et al. 1998). It is less clear whether neurons in layer I, like those in the ontogenetically related subplate, also directly contribute to the formation of the adult cortical circuitry, although there are some indications that they may. The dense, CR-derived horizontal plexus in layer I has been thought to provide a diffuse, background level of excitability (Schwartz et al. 1998). This might be important for the establishment of connections in layer I, much as the connections from the subplate to overlying cortical layers are necessary for the successful ingrowth of thalamocortical connections (Finney et al. 1998; Super et al. 1998). More recently, correlated spontaneous activity has been demonstrated in complex spatiotemporal patterns among NCR cells in the postnatal rat somatosensory cortex (Schwartz et al. 1998). Elsewhere in the nervous system, such activity has been thought to play a major role in the organization of neural circuitry (Katz and Shatz 1996).

There are several investigations of the development of cortical connections in areas 17 and 18 of the human (Burkhalter 1993; Burkhalter et al. 1993). DiI injections in postmortem material indicate that both the formation of local intrinsic connections within the superficial layers of area 17 and the ingrowth of feedback connections from area 18 to layer I of area 17 occur late. In particular, they are delayed relative to the formation in area 18 of local intrinsic connections and feedforward connections from area 17 to layer IV. Possibly, the greater density of Parv-ir NCR neurons in area 17 in the newborn may correlate with the delayed establishment of connectivity in the superficial layers. More data on connectional timetables in other areas and their relation to processes in layer I are necessary to address these issues.

Acknowledgements We thank Pope Yamada, Tina Knutson, and Diane Topinka for assisting with photographs and manuscript preparation, and Dr. Gary Van Hoesen for critical discussion and commentary. This work was supported by NINDS (NS 19632) and the Ministry of Health Foundation of China.

References

Alcantara S, Ferrer I (1994) Postnatal development of parvalbumin immunoreactivity in the cerebral cortex of the cat. J Comp Neurol 348:133–149

Alcantara S, Ferrer I, Soriano E (1993) Postnatal development of parvalbumin and calbindin D28k immunoreactivities in the cerebral cortex of the rat. Anat Embryol 188:63–73

Anderson JC, Martin KAC, Picanco-Diniz CW (1992) The neurons in layer I of cat visual cortex. Proc R Soc Lond B Biol Sci 248:27–33

Belichenko PV, Vogt Weisenhorn DM, Myklossy J, Celio MR (1995) Calretinin-positive Cajal-Retzius cells persist in the adult human neocortex. Neuroreport 6:1869–1874

Blumcke I, Hof PR, Morrison JH, Celio MR (1990) Distribution of parvalbumin immunoreactivity in the visual cortex of old world monkeys and humans. J Comp Neurol 301:417–432

Bradford R, Parnavelas JG, Lieberman AR (1977) Neurons in layer I of the developing occipital cortex of the rat. J Comp Neurol 176:121–132

Burkhalter A (1993) Development of forward and feedback connections between areas V1 and V2 of human visual cortex. Cereb Cortex 3:476–487

Burkhalter A, Bernardo KL, Charles V (1993) Development of local circuits in human visual cortex. J Neurosci 13:1916–1931

Cajal-Agueras SR, Lopez-Mascaraque L, Ramo C, Contamina-Gonzalvo P, De Carlos JA (1989) Layers I and VI of the visual cortex in the rabbit. A correlated Golgi and immunocytochemical study of somatostatin and vasoactive intestinal peptide containing neurons. J Hirnforsch 30:163–173

Cao QL, Yan XX, Luo XG, Garey LJ (1996) Prenatal development of parvalbumin immunoreactivity in the human striate cortex. Cereb Cortex 6:620–630

Celio MR, Baier W, Scharer L, De Viragh PA, Gerday C (1988) Monoclonal antibodies directed against the calcium binding protein parvalbumin. Cell Calcium 9:81–86

DeFelipe J, Jones EG (1988) Cajal on the cerebral cortex. Oxford University Press, New York

Del-Rio MR, DeFelipe J (1996) Colocalization of calbindin D28k, calretinin, and GABA immunoreactivities in neurons of the human temporal cortex. J Comp Neurol 369:472-482

Ding SL, Zheng DS, Yan YH, Sun WW, Guo QX (1996) Prenatal development of calbindin- and parvalbumin-immunoreactive structures in the primary auditory, somatosensory and motor cortices of the human brain. Acta Histochem Cytochem [Suppl] 29:1035–1036

Ding SL, Zheng DS, Yan YH, Sun WW, Guo QX (1997) Development of calbindin-containing neurons in the primary visual cortex of human fetus. Chin J Neuroanat 13:235–240

Ding SL, Zheng DS, Yan YH, Sun WW (1988) Prenatal development of parvalbumin containing neurons in human primary visual cortex. Acta Anat Sinica 29:45–49

Ding SL, Sun WW, Zheng DS, Yan YH (1999) Distribution and development of parvalbumin immunoreactive neurons in the hippocampal formation of human fetus. Acta Anat Sinica 30:133–135

Finney EM, Stone JR, Shatz CJ (1998) Major glutaminergic projection from subplate into visual cortex during development. J Comp Neurol 398:105–118

Fonseca M, Soriano E (1995) Calretinin-immunoreactive neurons in the normal human temporal cortex and in Alzheimer's disease. Brain Res 691:83–91

Frotscher M (1998) Cajal-Retzius cells, reelin and the formation of layers. Curr Opin Neurobiol 8:570–575

Gabbott PL, Jays PR, Bacon SJ (1997) Calretinin neurons in human medial prefrontal cortex (areas 24a, b, c, 32′, and 25). J Comp Neurol 381:389–410

Hashikawa T, Molinari M, Rausell E, Jones EG (1995) Patchy and laminar terminations of medial geniculate axons in monkey auditory cortex. J Comp Neurol 362:195–208

Heizmann CW, Braun K (1995) Calcium regulation by calcium binding proteins in neurodegenerative diseases. Springer, Berlin Heidelberg New York

Hendrickson AE, Van Brederode JFM, Mulligan KA, Celio MR (1991) Development of the calcium-binding proteins parvalbumin and calbindin-D28k in monkey striate cortex. J Comp Neurol 307:626–646

Hestrin S, Armstrong WE (1996) Morphology and physiology of cortical neurons in layer I. J Neurosci 16:5290–5300

Hof PR, Mufson EJ, Morrison JH (1995) Human orbitofrontal cortex: cytoarchitecture and quantitative immunohistochemical parcellation. J Comp Neurol 359:48–68

Huntley GW, Jones EG (1990) Cajal-Retzius cells in the developing monkey neocortex show immunoreactivity for calcium-binding proteins. J Neurocytol 19:200-212

Huttenlocher PR, Dabholkar AS (1997) Regional differences in synaptogenesis in human cerebral cortex. J Comp Neurol 387: 167–178

Katz L, Shatz CJ (1996) Synaptic activity and the construction of the cortical circuits. Science 274:1113–1138

Klekamp J, Riedel A, Harper C, Kretschmann HJ (1991) Quantitative changes during the postnatal maturation of the human visual cortex. J Neurol Sci 103:136–143

Krmpotic-Nemanic J, Kostovic I, Vidic Z, Nemanic D, Kostovic-Knezevic L (1987) Development of Cajal-Retzius cells in the human auditory cortex. Acta Otolaryngol 103: 477–480

Letinic K, Kostovic I (1998) Postnatal development of calcium-binding proteins calbindin and parvalbumin in human visual cortex. Cereb Cortex 8:660–669

Marin-Padilla M (1984) Neurons of layer I: A developmental analysis. In: Peters A, Jones EG (eds) Cerebral cortex, vol 1. Plenum Press, New York, pp 447–478

Marin-Padilla M (1990) Three-dimensional structural organization of layer I of the human cerebral cortex: a Golgi study. J Comp Neurol 299:89–105

Marin-Padilla M (1998) Cajal-Retzius cells and the development of the neocortex. Trends Neurosci 21:64–71

Marin-Padilla M, Marin-Padilla T (1982) Origin, prenatal development and structural organization of layer I of the human cerebral (motor) cortex. A Golgi method. Anat Embryol 164: 161–206

Meyer G, Gonzalez-Hernandez T (1993) Developmental changes in layer I of the human neocortex during prenatal life: A DiI-tracing and AChE and NADPH-d histochemistry study. J Comp Neurol 338:317–336

Meyer G, Goffinet AM (1998) Prenatal development of reelin-immunoreactive neurons in the human neocortex. J Comp Neurol 397:29–40

Prieto JJ, Peterson BA, Winer JA (1994) Morphology and spatial distribution of GABA-ergic neurons in cat primary auditory cortex (AI). J Comp Neurol 344:349–382

Saper CB (1996) Any way you cut it: a new journal policy for the use of unbiased counting methods. J Comp Neurol 364:5

Schwartz TH, Rabinowitz D, Vnni V, Kumar VS, Smetters DK, Tsiola A, Yuste R (1998) Networks of coactive neurons in developing layer I. Neuron 20:541–552

Seress L, Gulyas AI, Ferrer I, Tunon T, Soriano E, Freund TF (1993) Distribution, morphological features, and synaptic connections of parvalbumin and calbindin-D28k immunoreactive neurons in the human hippocampal formation. J Comp Neurol 337:208-230

Super HP, Soriano E, Uylings HBM (1998) The functions of the preplate in development and evolution of the neocortex and hippocampus. Brain Res Rev 27:40–64

Thomaidou D, Mione MC, Cavanagh JF, Parnavelas JG (1997) Apoptosis and its relation to the cell cycle in the developing cerebral cortex. J Neurosci 17:1075–1085

Verney C, Derer P (1995) Cajal-Retzius neurons in human cerebral cortex at midgestation show immunoreactivity for neurofilament and calcium-binding proteins. J Comp Neurol 359: 144–153

Yan XX, Cao QL, Luo XG, Garey LJ (1997) Prenatal development of calbindin-D28k immunoreactivity in human visual cortex. Cereb Cortex 7:57–62

Yan YH, Zheng DS, Ding SL, Sun WW (1993) An immunohistochemical study of parvalbumin-containing neurons in the cerebral cortex of human newborn. Chin J Histochem Cytochem 2:25–30

Yan YH, Van Brederode JFM, Hendrickson AE (1995) Transient colocalization of calretinin, parvalbumin, and calbindin-D28k in developing visual cortex of monkey. J Neurocytol 24:825–837

Zhou FM, Hablitz JJ (1996) Morphological properties of intracellularly labeled layer I neurons in rat neocortex. J Comp Neurol 376:198–213